

# Strange matter in rotating compact stars

Sarmistha Banik<sup>(a)</sup>, Matthias Hanauske<sup>(b)</sup> and Debades Bandyopadhyay<sup>(a)</sup>

<sup>(a)</sup>Saha Institute of Nuclear Physics, 1/AF Bidhannagar, Calcutta 700 064, India

<sup>(b)</sup>Institut für Theoretische Physik, J. W. Goethe Universität, D-60054 Frankfurt am Main, Germany

**Abstract.** We have constructed equations of state involving various exotic forms of matter with large strangeness fraction such as hyperon matter, Bose-Einstein condensates of antikaons and strange quark matter. First order phase transitions from hadronic to antikaon condensed and quark matter are considered here. The hadronic phase is described by the relativistic field theoretical model. Later those equations of state are exploited to investigate models of uniformly rotating compact stars. The effect of rotation on the third family branch for the equation of state involving only antikaon condensates is investigated. We also discuss the back bending phenomenon due to a first order phase transition from  $K^-$  condensed to quark matter.

## 1. Introduction

Neutron stars are born in type II supernova explosions of massive stars [1]. The matter in the neutron star interior is highly dense and cold. The matter density could exceed by a few times normal nuclear matter density. Exotic components of matter such as hyperons, antikaon condensates and quarks may appear there. Such a dense and cold matter can not be found in laboratories. Therefore, neutron stars are very useful laboratories to study the properties of dense matter [2, 3].

It is a challenging problem to constrain the equation of state (EoS) of dense matter in neutron stars. The theoretical investigation of mass-radius (M-R) relationship of compact stars is important because this can be directly compared with observations. Consequently, the composition and EoS of dense matter may be probed. Though accurate masses have been measured for several neutron stars in radio pulsar binaries, we do not have enough informations about their radii. Observations of thermal x-ray and optical radiation from isolated neutron stars such as RX J185635-3754, may provide informations about their radii [4]. Another interesting candidate for radius measurement is x-ray bursters. Cottam et al. [5] estimated the gravitational redshift  $z = 0.35$  of three spectral lines in x-ray bursts from EXO 0748-676. Recently, Villarreal and Strohmayer detected a 45 Hz rotational frequency for the same star [6]. These observations lead to a radius of 9.5-15 km and mass  $1.5-2.3M_{solar}$  for EXO 0748-676 [6]. It is now being argued that the measurement of moment inertia of star A in double pulsar system PSR J0737-3039 where masses have been determined already, could give an accurate estimate of the radius and put important constrain on the properties of neutron star matter [7].

Here we discuss various exotic forms of matter and their influence on equations of state and structures of static and rotating compact stars. In this context, we also report a new class of superdense stars called the third family in static [8, 9, 10, 11, 12, 13] as well as rotating configurations [14] and the back bending phenomenon [2, 3, 14, 15] which could be a signature for a first order phase transition in the neutron star interior. In section 2, we describe the calculation of EoS and structure of compact stars. Results are discussed in section 3. And the outlook is presented in section 4.

## 2. Model

Here we describe models of static and rotating compact stars. Such models are constructed by solving Einstein's field equations,

$$G^{\mu\nu} = R^{\mu\nu} - \frac{1}{2}g^{\mu\nu}R = 8\pi T^{\mu\nu}, \quad (1)$$

where  $R^{\mu\nu}$  is the Ricci tensor,  $g^{\mu\nu}$  is the space-time metric,  $R$  is the scalar curvature and  $T^{\mu\nu}$  is the energy-momentum tensor. The EoS is encoded in the energy-momentum tensor. The equilibrium structures of non-rotating stars are calculated from Tolman-Oppenheimer-Volkoff (TOV) equations. Here we are interested in the equilibrium structures of rotating compact stars. In this case, the metric has the form [16, 17]

$$ds^2 = -e^{\gamma+\rho}dt^2 + e^{2\alpha}(dr^2 + r^2d\theta^2) + e^{\gamma-\rho}r^2\sin^2\theta(d\phi - \omega dt)^2, \quad (2)$$

where metric functions depend on  $r$  and  $\theta$ . Angular velocity of local inertial frames is denoted by  $\omega$ .

In the following paragraphs, we discuss two equations of state for dense matter. In the first case (case I), we consider a first order phase transition from hadronic matter including hyperons to  $K^-$  condensed matter followed by a second order  $K^0$  condensation. In the other case (case II), we have first order phase transitions from nuclear to  $K^-$  condensed matter and then to quark matter.

For case I, we have hadronic phase, antikaon condensed phase and a mixed of those two phases. The constituents of matter in the hadronic phase are all the species of the baryon octet, electrons and muons. Baryon-baryon interaction is mediated by the exchange of scalar and vector mesons. Here we adopt a relativistic field theoretical model to describe hadronic and antikaon condensed phase. The model is also extended to include hyperon-hyperon interaction through two additional strangeness meson  $f_0(975)$  (hereafter denoted as  $\sigma^*$ ) and  $\phi(1020)$ . Therefore the Lagrangian density for baryon-baryon interaction is [10, 11, 18]

$$\begin{aligned} \mathcal{L}_B = & \sum_B \bar{\psi}_B (i\gamma_\mu \partial^\mu - m_B + g_{\sigma B}\sigma - g_{\omega B}\gamma_\mu \omega^\mu - g_{\rho B}\gamma_\mu \mathbf{t}_B \cdot \boldsymbol{\rho}^\mu) \psi_B \\ & + \sum_B \bar{\psi}_B (g_{\sigma^* B}\sigma^* - g_{\phi B}\gamma_\mu \phi^\mu) \psi_B \\ & + \frac{1}{2} (\partial_\mu \sigma \partial^\mu \sigma - m_\sigma^2 \sigma^2) - U(\sigma) + \frac{1}{2} (\partial_\mu \sigma^* \partial^\mu \sigma^* - m_{\sigma^*}^2 \sigma^{*2}) \\ & - \frac{1}{4} \omega_{\mu\nu} \omega^{\mu\nu} + \frac{1}{2} m_\omega^2 \omega_\mu \omega^\mu - \frac{1}{4} \boldsymbol{\rho}_{\mu\nu} \cdot \boldsymbol{\rho}^{\mu\nu} + \frac{1}{2} m_\rho^2 \boldsymbol{\rho}_\mu \cdot \boldsymbol{\rho}^\mu \\ & - \frac{1}{4} \phi_{\mu\nu} \phi^{\mu\nu} + \frac{1}{2} m_\phi^2 \phi_\mu \phi^\mu. \end{aligned} \quad (3)$$

The scalar self-interaction term is

$$U(\sigma) = \frac{1}{3}g_2\sigma^3 + \frac{1}{4}g_3\sigma^4. \quad (4)$$

The antikaon condensed phase is composed of baryons of the octet embedded in the condensate, electrons and muons. Similarly, we adopt a relativistic field theoretical approach for the description of (anti)kaon-baryon interaction. Here (anti)kaon-baryon interaction is treated in the same footing as baryon-baryon interaction. The Lagrangian density for (anti)kaons in the minimal coupling scheme is [10, 11, 19]

$$\mathcal{L}_K = D_\mu^* \bar{K} D^\mu K - m_K^{*2} \bar{K} K, \quad (5)$$

where the covariant derivative  $D_\mu = \partial_\mu + ig_{\omega K}\omega_\mu + ig_{\phi K}\phi_\mu + ig_{\rho K}t_K \cdot \boldsymbol{\rho}_\mu$ . The isospin doublet for kaons is denoted by  $K \equiv (K^+, K^0)$  and that for antikaons is  $\bar{K} \equiv (K^-, \bar{K}^0)$ . The effective mass of (anti)kaons in this minimal coupling scheme is given by

$$m_K^* = m_K - g_{\sigma K}\sigma - g_{\sigma^* K}\sigma^*, \quad (6)$$

In the mean field approximation adopted here, the meson fields are replaced by their expectation values. The mean meson fields are denoted by  $\sigma, \sigma^*, \omega_0, \phi_0$  and  $\rho_{03}$ . Each meson field equation in the antikaon condensed phase has contributions from antikaon condensates [10, 11]. These equations differ from those of pure hadronic phase by the antikaon condensate terms.

The in-medium energies of antikaon for  $s$ -wave ( $\mathbf{k} = \mathbf{0}$ ) is

$$\omega_{K^-, \bar{K}^0} = m_K^* - g_{\omega K}\omega_0 - g_{\phi K}\phi_0 \mp \frac{1}{2}g_{\rho K}\rho_{03}, \quad (7)$$

where the isospin projection  $I_{3\bar{K}} = \mp 1/2$  for  $K^-$  meson and  $\bar{K}^0$  meson respectively. The onsets of antikaon condensations are given by [10, 11],

$$\mu_{K^-} = \mu_e, \quad (8)$$

$$\mu_{\bar{K}^0} = 0, \quad (9)$$

where  $\mu_{K^-}$  and  $\mu_{\bar{K}^0}$  are respectively the chemical potentials of  $K^-$  and  $\bar{K}^0$ .

The energy density ( $\epsilon^h$ ) and pressure ( $P^h$ ) in hadronic phase are related by  $P^h = \sum_i \mu_i n_i - \epsilon^h$ . Similarly, the pressure in the antikaon condensed phase follows from the relation  $P^{\bar{K}} = \sum_i \mu_i n_i - \epsilon^{\bar{K}}$ , where  $n_i$  is the number density of  $i$ -th species. The expressions for  $\epsilon^h$  and  $\epsilon^{\bar{K}}$  are given as in Ref. [11].

The mixed phase of antikaon condensed matter and hadronic matter is governed by Gibbs phase rules and global conservation laws [2]. The Gibbs phase rules read,  $P^h = P^{\bar{K}}$  and  $\mu_B^h = \mu_B^{\bar{K}}$  where  $\mu_B^h$  and  $\mu_B^{\bar{K}}$  are chemical potentials of baryon B in hadronic and  $K^-$  condensed matter respectively. The conditions for global charge neutrality and baryon number conservation are  $(1 - \chi)Q^h + \chi Q^{\bar{K}} = 0$  and  $n_B = (1 - \chi)n_B^h + \chi n_B^{\bar{K}}$  where  $\chi$  is the volume fraction in the condensed phase. Charges in hadronic and  $K^-$  condensed phase are  $Q^h = \sum_B q_B n_B^h - n_e - n_\mu$  and  $Q^{\bar{K}} = \sum_B q_B n_B^{\bar{K}} - n_{K^-} - n_e - n_\mu$  respectively, where  $n_B^h$  and  $n_B^{\bar{K}}$  are the number density of baryon B in pure hadronic and antikaon condensed phase and  $n_{K^-}, n_e$  and  $n_\mu$  are number densities of antikaons, electrons and muons respectively. The total energy density in the mixed phase is given by  $\epsilon = (1 - \chi)\epsilon^h + \chi\epsilon^{\bar{K}}$ .

For case II, the first order phase transition from nuclear matter to  $K^-$  condensed matter is treated in the same prescription as it is described above. However, the hadronic and antikaon condensed phases are composed of neutrons, protons, electrons

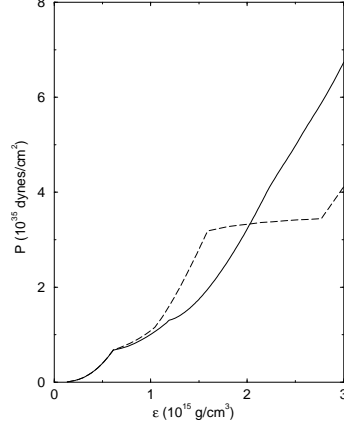


**Figure 1.** The equation of state, pressure  $P$  versus energy density  $\varepsilon$ , for two cases as described in the text.

and muons. In this case, we also consider a first order phase transition from antikaon condensed matter to quark matter. The pure quark matter is composed of  $u$ ,  $d$  and  $s$  quarks. We describe the EoS of pure quark matter in the MIT bag model [20]. The free energy density of non-interacting quarks is given by,

$$\Omega = \frac{3}{\pi^2} \sum_{i=u,d,s} \int_0^{p_{F,i}} dp p^2 (\sqrt{p^2 + m_i^2} - \mu_i) + B, \quad (10)$$

where  $B$  is the bag energy density. The pressure in the quark phase is given by  $P^Q = -\Omega$  and the energy density ( $\epsilon^Q$ ) is obtained from the Gibbs-Duhem relation. And the mixed phase is governed by the Gibbs phase rules and conservation laws.

### 3. Results & Discussions

In this calculation, we adopt GM1 parameter set [21] where nucleon-meson coupling constants are determined from the nuclear matter saturation properties. The vector meson coupling constants for (anti)kaons and hyperons are determined from the quark model [18] whereas the scalar meson coupling constants for hyperons and antikaons are obtained from the potential depths of hyperons and antikaons in normal nuclear matter [11, 18]. As the phenomenological fit to the  $K^-$  atomic data yielded a very strong real part of antikaon potential  $U_{\bar{K}} = -180 \pm 20$  MeV [22], we perform this calculation with an antikaon optical potential of -160 MeV at normal nuclear matter density ( $n_0 = 0.153 fm^{-3}$ ). The coupling constants for strange mesons with hyperons and (anti)kaons are taken from Ref.[11, 18]. Also, we consider a bag constant  $B^{1/4} = 200$  MeV and strange quark mass  $m_s = 150$  MeV for quark EoS in case II.

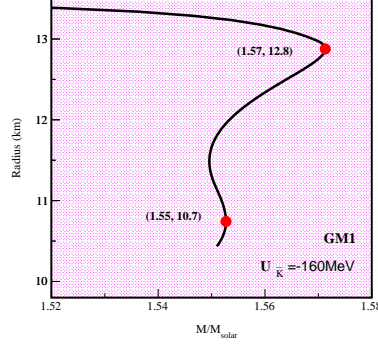


**Figure 2.** Mass-radius relationship of non-rotating stars calculated with the equation of state for case I.

The equations of state, pressure versus energy density, for case I and case II are exhibited in Figure 1 by solid and dashed lines respectively. For both cases, the upper and lower boundaries of the mixed phase of hadronic and  $K^-$  condensed matter are identified by two kinks. The mixed phase begins at energy density  $\epsilon = 6.11 \times 10^{14}$  g/cm<sup>3</sup> (or  $2.23n_0$ ). For case I,  $\Lambda$  hyperons are populated in the mixed phase at  $2.51n_0$  whereas  $\Xi^-$  and  $\Sigma^-$  hyperons are populated at much higher densities. A second order  $K^0$  condensation occurs in case I just after the mixed phase is over at  $\epsilon = 1.17 \times 10^{15}$  g/cm<sup>3</sup>. For case II, the phase transition to quark matter is delayed due to the early onset of  $K^-$  condensation depending on the parameters. The first order  $K^-$  condensed-quark matter phase transition begins at  $\epsilon = 1.59 \times 10^{15}$  g/cm<sup>3</sup> and ends at  $\epsilon = 2.77 \times 10^{15}$  g/cm<sup>3</sup>. In this case, the extent of the mixed phase is quite large. We note that the overall EoS for case I is softer than that of case II.

In Figure 2, the mass-radius relationship of non-rotating stars is displayed for the EoS of case I. The filled circles correspond to the maximum masses. We obtain a maximum neutron star mass of  $1.57M_{solar}$  corresponding to a radius of 12.8 km as shown in the figure. It is found that after the positive slope neutron star branch, there is an unstable region followed by another positive slope compact star branch. This new branch of compact stars is the result of the discontinuity in the speed of sound due to the kinks or first order phase transition in the EoS for case I. This new sequence of superdense stars beyond the neutron star branch is called the third family branch. From the study of fundamental mode of radial vibration, it was found that the third family branch was a stable one [11]. The compact stars in the third family branch have different compositions and smaller radii than their counterparts on the neutron star branch [11, 13]. The maximum mass of the compact star in the third family branch is  $1.55M_{solar}$  corresponding to a radius 10.7 km.

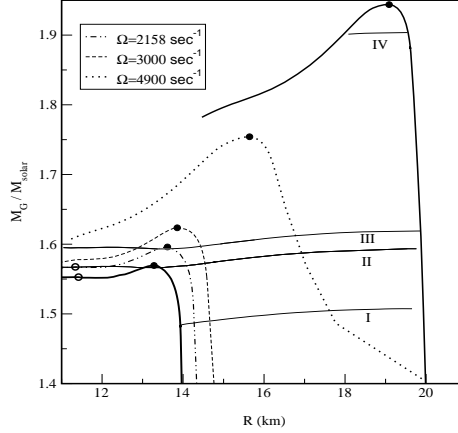


**Figure 3.** Gravitational mass as a function of equatorial radius for case I. The static and mass shedding limit sequences along with fixed angular velocity sequences are displayed here. Also, normal and supramassive sequences are plotted.

Now we discuss the mass-equatorial radius relationship of rotating sequences calculated with the EoS of case I. This is shown in Figure 3. In the preceding paragraph, we have discussed the third family of compact stars in the static sequence calculated with this EoS. It is interesting to watch what happens to this third family branch in rotating cases. In Figure 3, the extreme left and right curves denote the static and mass shedding limit sequences. Each compact star on the mass shedding limit rotates with a maximum frequency called the Kepler frequency and it becomes unstable beyond this frequency. Fixed angular velocity curves are also shown in this figure. On each curve, the maximum mass in the neutron star branch is denoted by solid circles whereas the maximum mass in the third family branch is represented by open circles. We observe that with increasing rotation, the maximum star masses also increase and are shifted to smaller central energy densities or larger radii. This is attributed to the presence of centrifugal force in rotating stars. On the other hand, we note that the third family of compact stars disappears beyond the fixed angular velocity curve  $\Omega = 2158 \text{ sec}^{-1}$ . The reason is the strengthening of the centrifugal force with increasing rotation. Consequently, fast rotating stars could not probe the high density part of the EoS which is responsible for the origin of a third family branch.

In Figure 3, we also plot fixed baryon number evolutionary sequences. Here two normal sequences are shown by curves I and II and two supramassive sequences by curves III and IV. Fixed baryon number sequences provide important informations about isolated rotating stars as they slow down with time due to the loss of energy

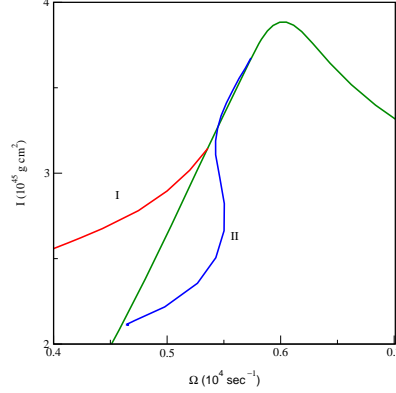


**Figure 4.** Moment of inertia ( $I$ ) is plotted with angular velocity ( $\Omega$ ) for the EoS of case II. Normal and supramassive sequences are shown by curves I and II respectively. The other curve is the mass shedding limit sequence.

and angular momentum through electromagnetic and gravitational radiation. We observe from the figure that non-rotating stars are the members of normal sequences. However, no member of supramassive sequences is a non-rotating compact star. When a supramassive star loses sufficient angular momentum such that the centrifugal support against self gravity is impossible, it would then collapse to a black hole. This was considered as a possible scenario for gamma ray bursts [23].

We also investigate the mass-equatorial radius relationship of the static, mass shedding limit and fixed angular velocity sequences calculated with the EoS for case II. However, we do not find any third family solution in the static and rotating cases. But we find some interesting results from the study of a supramassive sequence. We display moment of inertia ( $I$ ) with angular velocity ( $\Omega$ ) in Figure 4. Curve I implies the normal sequence with baryon number  $N_b = (2.15 \times 10^{57})$  whereas curve II is a supramassive sequence with  $N_b = (2.45 \times 10^{57})$ . The other curve is the mass shedding limit sequence. For the normal sequence, the moment of inertia always decreases with decreasing angular velocity. However, curve II exhibits that after the initial spin down of the neutron star along this sequence, there is a spin up followed by another spin down. This is known as the back bending phenomenon. We observe that this back bending phenomenon is the result of the first order phase transition from antikaon condensed to quark matter. It is worth mentioning here that the supramassive neutron star is stable on the back bending segment [14]. We also note that the period of the neutron star in the back bending part varies from 1.10 ms to 1.35 ms corresponding to the variation in angular velocity from  $5700 \text{ s}^{-1}$  to  $4660 \text{ s}^{-1}$ . The minimum observed pulsar period is so far 1.56 ms. Future pulsar surveys would tell us whether pulsars rotating faster than the currently known one exist in nature or not.

#### 4. Outlook

We have investigated equations of state including exotic forms of matter and computed the structures of static and rotating compact stars. Many interesting results such as the third family of compact stars containing exotic matter, the back bending effect which could signal a first order phase transition in the neutron star interior, are obtained here. Our results are sensitive to input parameters such as antikaon optical potential depth and bag constant. Future experiments on deeply bound states of antibaryon-nucleus at GSI, Germany and  $\bar{K}$ -nucleus at Japan Proton Accelerator Complex (J-PARC) will provide opportunity to investigate dense and cold matter in laboratories and determine those parameters accurately. It would be possible to constrain the composition and EoS of dense and cold matter in compact stars from observations and experiments in future.

#### Acknowledgments:

This work is supported by the Department of Science and Technology (DST), Government of India, German Academic Exchange Service (DAAD), Germany, Department of Science of Technology, Government of South Africa and GSI, Germany.

#### References

- [1] Bethe H A 1990 Rev. Mod. Phys. **62** 801
- [2] Glendenning N K 1997 Compact stars (New York, Springer)
- [3] Weber F 1999 Pulsars as Astrophysical Laboratories for Nuclear and Particle Physics (Bristol and Philadelphia, Institute of Physics Publishing)
- [4] Walter F M and Lattimer J M 2002 Astrophys. J. **576** L145  
Drake J J et al. 2002 Astrophys. J. **572** 996
- [5] Cottam J, Paerels F and Mendez M 2002 Nature **420** 51  
Miller C 2002 Nature **420** 31
- [6] Villarreal A R and Strohmayer T E 2004 astro-ph/0409584
- [7] Morrison I A, Baumgarte T W, Shapiro S L and Pandharipande V R 2004 astro-ph/0411353  
Lattimer J M and Schutz B F 2004 astro-ph/0411470
- [8] Glendenning N K and Kettner C 2000 Astron. Astrophys. **353** L9
- [9] Schertler K, Greiner C, Schaffner-Bielich J and Thoma M H 2000 Nucl. Phys. **A677** 463
- [10] Banik S and Bandyopadhyay D 2001 Phys. Rev. C **63** 035802
- [11] Banik S and Bandyopadhyay D 2001 Phys. Rev. C **64** 055805
- [12] Schaffner-Bielich J, Hanauske M, Stöcker H and Greiner W 2002 Phys. Rev. Lett. **89** 171101
- [13] Banik S and Bandyopadhyay D 2003 Phys. Rev. D **67** 123003
- [14] Banik S, Hanauske M, Bandyopadhyay D and Greiner W 2004 Phys. Rev. D **70** 123004
- [15] Zdunik J L, Haensel P, Gourgoulhon E and Bejger M 2004 Astron. Astrophys. **416** 1013
- [16] Cook G B, Shapiro S L and Teukolsky S A 1994 Astrophys. J. **422** 227
- [17] Stergioulas N and Friedman J L 1995 Astrophys. J. **444** 306
- [18] Schaffner J and Mishustin I N 1996 Phys. Rev. C **53** 1416
- [19] Glendenning N K and Schaffner-Bielich J 1998 Phys. Rev. Lett. **81** 4564
- [20] Farhi E and Jaffe R L 1984 Phys. Rev. D **30** 2379
- [21] Glendenning N K and Moszkowski S A 1991 Phys. Rev. Lett. **67** 2414
- [22] Friedman E, Gal A, Mareš J and Cieplý A 1999 Phys. Rev. C **60** 024314
- [23] Vietri M and Stella L 1999 Astrophys. J. **527** L43